J. Lindberg, T. Setälä, M. Kaivola, and A. T. Friberg, Degree of polarization in light transmission through a near-field probe, Journal of Optics A: Pure and Applied Optics 6, S59-S63 (2004).

INSTITUTE OF PHYSICS PUBLISHING JOURNAL OF OPTICS A: PURE AND APPLIED OPTICS

J. Opt. A: Pure Appl. Opt. **6** (2004) S59–S63 PII: S1464-4258(04)69151-3

Degree of polarization in light transmission through a near-field probe

J Lindberg[1], **T Setälä**[1], **M Kaivola**[1] **and A T Friberg**[2]

[1] Department of Engineering Physics and Mathematics, Helsinki University of Technology, PO Box 2200, FIN-02015 HUT, Finland
[2] Department of Microelectronics and Information Technology, Royal Institute of Technology, SE-164 40 Kista, Sweden

E-mail: jlindber@cc.hut.fi

Received 17 September 2003, accepted for publication 8 January 2004
Published 24 February 2004
Online at stacks.iop.org/JOptA/6/S59 (DOI: 10.1088/1464-4258/6/3/010)

Abstract
We analyse the changes in the partial polarization of random, stationary light fields in transmission through a near-field probe. The probe is modelled as a two-dimensional metal-coated optical fibre tip through which the field is propagated by applying the boundary-integral method. Both the magnitude of the opening angle and the aperture size of the probe are found to significantly influence the partial polarization of the field. We discuss the results in terms of both the conventional two-dimensional and the recent three-dimensional formalism for the degree of polarization.

Keywords: optical near field, degree of polarization, boundary-integral method

1. Introduction

The polarization properties of optical near fields have attracted considerable attention in recent years. The polarization state is of crucial importance in many applications of nanophotonics such as near-field microscopy, which has enabled optical imaging of nanoscale structures [1, 2]. In a common mode of near-field microscopy, a nanoprobe consisting of a metal-coated tapered optical fibre tip with a sub-wavelength aperture at the apex is scanned very close to the sample. The light emitted or scattered by the sample is collected by the probe, or the probe illuminates the sample and the scattered field is detected in the far zone. Several theoretical methods have been employed to analyse the electromagnetic interaction between the sample and the probe in the near field [3–6]. In particular, the coupling of the different field components into the probe [7, 8] and the role of polarization in near-field image formation [9–11] have been extensively studied. However, the theoretical studies, as a rule, deal with monochromatic, fully polarized fields, although near-field measurements using partially coherent, partially polarized light might in some cases be more relevant [10].

In this paper we analyse the changes in the partial polarization of light fields in transmission through a near-field probe. We apply the boundary-integral method to rigorously propagate the electromagnetic field through a two-dimensional metal-coated fibre tip used as a model for the near-field probe [6]. In particular, we investigate the influence of the tip's opening angle and the size of the output aperture on the polarization state of the transmitted light using the recently introduced three-dimensional degree of polarization. Furthermore, by considering the far field, we demonstrate that the three-dimensional and the usual two-dimensional formalisms for the degree of polarization lead to the same conclusions on the changes in the polarization state.

The paper is organized as follows: in section 2 we recall the relevant aspects of the two- and three-dimensional formalisms for the degree of polarization. In section 3 the model probe is presented and the boundary-integral method is briefly outlined. The results of our calculations are presented and discussed in section 4, and the main conclusions are summarized in section 5.

2. Degree of polarization for near fields

The degree of polarization is a fundamental quantity that characterizes the correlations between the electric field components of a random electromagnetic field. The usual formulation of the degree of polarization is valid only for paraxial waves, which are expressible by two orthogonal electric field components [12]. In the following, we consider

such a field propagating along the y-axis with the electric field vector lying in the xz-plane. The two-dimensional degree of polarization, $P_2(\boldsymbol{r}, \omega)$, at a point $\boldsymbol{r}$, at frequency ω, is then written as

$$P_2^2(\boldsymbol{r}, \omega) = 1 - \frac{4 \det[\Phi_2(\boldsymbol{r}, \omega)]}{\mathrm{tr}^2[\Phi_2(\boldsymbol{r}, \omega)]}, \tag{1}$$

where det and tr stand for the determinant and the trace respectively, and $\Phi_2(\boldsymbol{r}, \omega)$ denotes the Hermitian, non-negative definite, 2×2 spectral coherence matrix, with its elements given by

$$\phi_{ij}(\boldsymbol{r}, \omega) = \langle E_i^*(\boldsymbol{r}, \omega) E_j(\boldsymbol{r}, \omega) \rangle, \qquad (i, j) = (x, z). \tag{2}$$

In this equation, $E_i(\boldsymbol{r}, \omega)$ and $E_j(\boldsymbol{r}, \omega)$ are the transverse electric-field components at $\boldsymbol{r}$ and the angle brackets and the asterisk denote averaging and complex conjugation, respectively. It can be shown that $0 \leqslant P_2(\boldsymbol{r}, \omega) \leqslant 1$, with 0 and 1 corresponding to fully unpolarized and to fully polarized light. More insight into the 2D degree of polarization is obtained by writing it in terms of the (complex) correlation coefficient between the field components, defined as

$$\begin{aligned} \mu_{xz}(\boldsymbol{r}, \omega) &\equiv \frac{\phi_{xz}(\boldsymbol{r}, \omega)}{[\phi_{xx}(\boldsymbol{r}, \omega)\phi_{zz}(\boldsymbol{r}, \omega)]^{1/2}}, \\ \mu_{zx}(\boldsymbol{r}, \omega) &= \mu_{xz}^*(\boldsymbol{r}, \omega). \end{aligned} \tag{3}$$

Using this definition the 2D degree of polarization assumes the form

$$P_2^2(\boldsymbol{r}, \omega) = 1 - \frac{4[1 - |\mu_{xz}(\boldsymbol{r}, \omega)|^2]\phi_{xx}(\boldsymbol{r}, \omega)\phi_{zz}(\boldsymbol{r}, \omega)}{[\phi_{xx}(\boldsymbol{r}, \omega) + \phi_{zz}(\boldsymbol{r}, \omega)]^2}. \tag{4}$$

Thus, $P_2^2(\boldsymbol{r}, \omega)$ is readily expressible in terms of the spectral densities of the two field components and the modulus of their correlation coefficient. It is straightforward to prove from equation (4) that [13]

$$P_2(\boldsymbol{r}, \omega) \geqslant |\mu_{xz}(\boldsymbol{r}, \omega)|. \tag{5}$$

In addition, the coordinate system can always be rotated about the field's direction of propagation in such a way that the spectral densities of the two field components become equal, i.e. $\phi_{xx}(\boldsymbol{r}, \omega) = \phi_{zz}(\boldsymbol{r}, \omega)$. In this particular case the equality sign in equation (5) holds and we obtain

$$P_2(\boldsymbol{r}, \omega) = |\mu_{xz}(\boldsymbol{r}, \omega)|. \tag{6}$$

Recently, the concept of the degree of polarization was extended to deal with general three-dimensional, non-paraxial electromagnetic fields [14]. The 3D degree of polarization, $P_3(\boldsymbol{r}, \omega)$, is given by the formula

$$P_3^2(\boldsymbol{r}, \omega) = \frac{3}{2}\left\{\frac{\mathrm{tr}[\Phi_3^2(\boldsymbol{r}, \omega)]}{\mathrm{tr}^2[\Phi_3(\boldsymbol{r}, \omega)]} - \frac{1}{3}\right\}, \tag{7}$$

where $\Phi_3(\boldsymbol{r}, \omega)$ denotes the 3×3 spectral coherence matrix for which the elements are given by equation (2), with indices $(i, j) = (x, y, z)$. The value of $P_3(\boldsymbol{r}, \omega)$ is bounded between 0 and 1, corresponding to fully unpolarized and fully polarized three-dimensional fields respectively. In analogy with equation (3), we may introduce the correlation coefficients between the three orthogonal field components, which allows us to rewrite $P_3(\boldsymbol{r}, \omega)$ in the form

$$P_3^2(\boldsymbol{r}, \omega) = 1 - \frac{\sum_{i,j} 3[1 - |\mu_{ij}(\boldsymbol{r}, \omega)|^2]\phi_{ii}(\boldsymbol{r}, \omega)\phi_{jj}(\boldsymbol{r}, \omega)}{[\phi_{xx}(\boldsymbol{r}, \omega) + \phi_{yy}(\boldsymbol{r}, \omega) + \phi_{zz}(\boldsymbol{r}, \omega)]^2}, \tag{8}$$

where the summation is carried out over index pairs $(ij) = (xy, xz, yz)$. Equation (8) expresses $P_3(\boldsymbol{r}, \omega)$ in terms of the absolute values of the correlations between the field components, and their spectral densities. Furthermore, equation (8) yields the following inequality [14]

$$P_3^2(\boldsymbol{r}, \omega) \geqslant \frac{\sum_{i,j} |\mu_{ij}(\boldsymbol{r}, \omega)|^2 \phi_{ii}(\boldsymbol{r}, \omega)\phi_{jj}(\boldsymbol{r}, \omega)}{\sum_{i,j} \phi_{ii}(\boldsymbol{r}, \omega)\phi_{jj}(\boldsymbol{r}, \omega)}, \tag{9}$$

where the summations again are performed over the index pairs $(ij) = (xy, xz, yz)$. Equation (9) shows that $P_3^2(\boldsymbol{r}, \omega)$ represents the upper limit of the averaged correlation coefficients squared, weighted by the corresponding spectral densities. Again, the coordinate system may always be rotated in three dimensions in such a way that the spectral densities become equal. In this coordinate system the equality sign in equation (9) holds and we have

$$P_3^2(\boldsymbol{r}, \omega) = \frac{|\mu_{xy}(\boldsymbol{r}, \omega)|^2 + |\mu_{xz}(\boldsymbol{r}, \omega)|^2 + |\mu_{yz}(\boldsymbol{r}, \omega)|^2}{3}, \tag{10}$$

which is the 3D analogue of equation (6).

We emphasize that the value of the degree of polarization depends, in general, on the dimensionality of the treatment. This fact is intuitively understood by considering the following plane-wave example. A plane wave, whether unpolarized in the usual two-dimensional sense or not, can never be fully unpolarized in the three-dimensional treatment [14], since the electric field vector of such a wave oscillates in a single plane. In other words, the possible states of the electric field in the statistical ensemble are confined to lie in the plane perpendicular to the propagation direction, and hence the randomness of the field components is strongly limited leading to a non-zero 3D degree of polarization. A more thorough discussion of this fact is found in [14].

3. Boundary-integral method

For the calculation, we employ a two-dimensional model for the near-field fibre tip illustrated in figure 1. The aluminium-coated structure is uniform in the z-direction and the medium in each region is assumed linear, homogeneous and isotropic. The fibre tip is of glass ($n_\mathrm{g} = 1.5$) and the ambient medium has an index of refraction of $n_\mathrm{a} = 1.0$. The thicknesses of the aluminium coatings ($n_\mathrm{Al} = 0.718 + 5.917\mathrm{i}$) in the horizontal layer and around the tip are 500 and 70 nm respectively. The horizontal aluminium layer is chosen to be thick enough in order that we can reasonably approximate that the field is zero on the lower border of the layer far away from the tip apex.

In the 2D geometry each realization of the electromagnetic field can be represented as a superposition of an s-polarized (transverse electric) and a p-polarized (transverse magnetic) component. The s-polarized wave is represented by a single electric field component which, in this case, points in the z-direction. For the p-polarized wave, on the other hand, a z-oriented magnetic field component is used. In both cases the

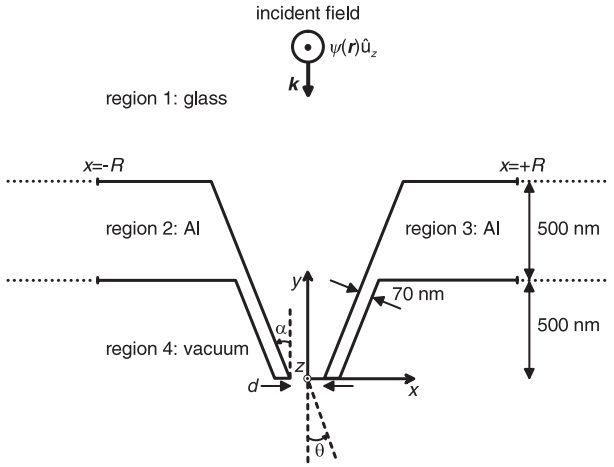

Figure 1. A 2D model for a metal-coated tapered fibre tip with an opening angle α and an output aperture diameter d. The geometry is similar to that investigated in [6]. The vertical distance between the lower and upper aperture is 1000 nm. The thickness of the aluminium layer is 500 nm in the horizontal part and 70 nm around the tip. A plane wave of wavelength $\lambda = 488$ nm and wavevector $\boldsymbol{k} \parallel -\hat{u}_y$ is incident on the structure. The scalar field $\psi(\boldsymbol{r})$ stands for the z component of the electric or the magnetic field vector, corresponding to s- or p-polarized light.

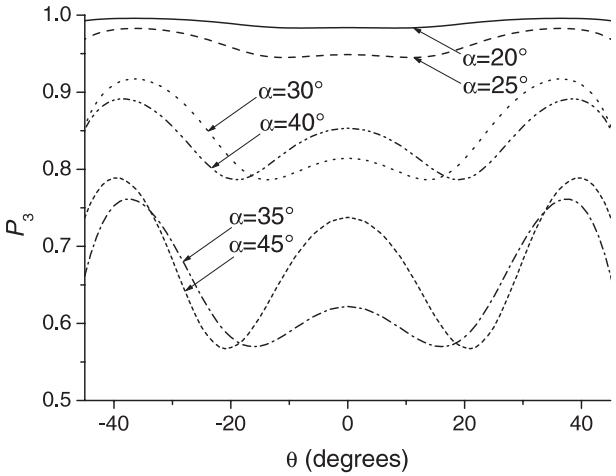

Figure 2. Behaviour of the 3D degree of polarization, P_3, as a function of angle θ at the distance $r = 10$ μm from the output aperture. The incident wave is fully unpolarized and the different curves correspond to varying opening angles of the tip.

behaviour of the electromagnetic field is everywhere governed by the 2D scalar Helmholtz equation

$$(\nabla^2 + k_0^2 n^2)\psi(\boldsymbol{r}) = 0, \tag{11}$$

where $\psi(\boldsymbol{r})$ denotes the (complex) amplitude of the electric (s polarization) or the magnetic field (p polarization). Further, k_0 is the free-space wavenumber, n is the refractive index of the medium and $\boldsymbol{r} = (x, y)$. In this work we make use of a numerical procedure known as the boundary-integral method to solve equation (11) in the arrangement of figure 1. Below we briefly outline the theory; for a more comprehensive presentation see, e.g., [6, 15–17].

The geometry of figure 1 consists of four regions. The solution of the Helmholtz equation in a region labelled by l ($l = 1, 2, 3, 4$) can be expressed as a boundary integral

$$\psi_l(\boldsymbol{r}) = \oint_{s_l} \{G_l(\boldsymbol{r}, \boldsymbol{r}')[\hat{n} \cdot \nabla'\psi_l(\boldsymbol{r}')] - \psi_l(\boldsymbol{r}')[\hat{n} \cdot \nabla' G_l(\boldsymbol{r}, \boldsymbol{r}')]\}\, \mathrm{d}s', \tag{12}$$

where $\hat{n}$ denotes the outward unit vector normal to the curve s_l around the region. The Green function $G_l(\boldsymbol{r}, \boldsymbol{r}')$, which satisfies the inhomogeneous 2D Helmholtz equation with a delta-function source term, is explicitly given by

$$G_l(\boldsymbol{r}, \boldsymbol{r}') = \frac{\mathrm{i}}{4} H_0^{(1)}(k_0 n_l |\boldsymbol{r} - \boldsymbol{r}'|), \tag{13}$$

where $H_0^{(1)}$ is a zero-order Hankel function of the first kind, and $\boldsymbol{r}$ and $\boldsymbol{r}'$ refer to the field and source points respectively.

None of the regions in the fibre-tip model is closed. However, to employ the boundary-integral method, the domains must to be closed and for this we adopt the following procedures [6]: the boundaries separating regions 1 and 2, and regions 2 and 4, are extended from $x = -R$ to $-\infty$. Similarly, the boundaries separating regions 1 and 3, and 3 and 4, are extended from $x = +R$ to $+\infty$. Domains 2 and 3 are then closed with vertical segments at $x = -\infty$ and $+\infty$ respectively, and infinite semicircles are used to close domains 1 and 4. For points in region 1, the integral over the semicircle gives the incident field [6], whereas the integral over the semicircle in region 4 vanishes due to the fact that the field satisfies the Sommerfeld radiation condition.

Calculation of the field inside a region using the boundary-integral method requires knowledge of the field and its normal derivative on the boundary. The boundary values are obtained by taking the limit of equation (12) as the field point $\boldsymbol{r}$ approaches the boundary. The boundaries in the interval $-R \leqslant x \leqslant +R$ are then discretized and the boundary conditions for the electric and magnetic fields are employed to relate the field and its normal derivative for the adjacent regions. After the contributions from the extended boundaries ($|x| > R$) are taken into account, the field and its normal derivative on the boundary are obtained by solving the ensuing matrix equation. Once the boundary values are known, the field inside a region can be calculated from equation (12). We note that in the case of the p-polarized light, where the magnetic field is known, the electric field is straightforwardly obtained by employing the Maxwell equations. The accuracy of the results is verified by an energy conservation check.

4. Results

We assume that the field incident on the structure shown in figure 1 is a planar wave, with equal spectral densities associated with the s and p components, but with a degree of polarization which may be arbitrary. According to equations (4) and (8), the 2D and 3D degrees of polarization can be expressed using the spectral densities and the correlation coefficients of the orthogonal field components. For the incident field these quantities are written as $\phi^{\mathrm{i}}_{xx}(\boldsymbol{r}, \omega) = \phi^{\mathrm{i}}_{zz}(\boldsymbol{r}, \omega)$, $\phi^{\mathrm{i}}_{yy}(\boldsymbol{r}, \omega) = 0$ and $0 \leqslant |\mu^{\mathrm{i}}_{xz}(\boldsymbol{r}, \omega)| = P_2(\boldsymbol{r}, \omega) \leqslant 1$. We represent the incident wave by an ensemble in which each realization has equal amplitudes in the s and p directions. On employing the boundary-integral method, we

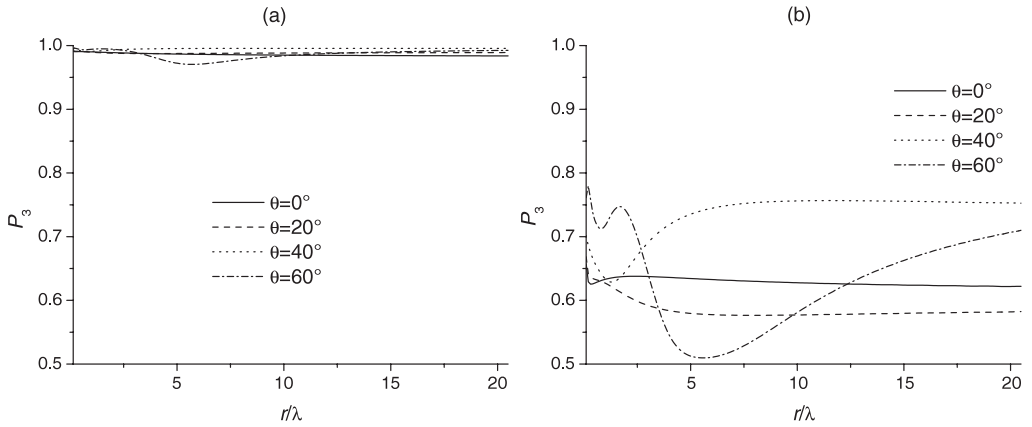

Figure 3. Behaviour of the 3D degree of polarization, P_3, as a function of the radial distance r from the aperture in four directions $\theta = 0°$, 20°, 40° and 60°. The incident wave is unpolarized and the opening angle of the probe tip is (a) $\alpha = 20°$ and (b) $\alpha = 35°$.

calculate the s- and p-polarized transmitted field distributions for a single realization. The s component leads to the intensity $\phi^{\mathrm{t}}_{zz}(\boldsymbol{r}, \omega)$, while the p component gives the averaged quantities $\phi^{\mathrm{t}}_{xx}(\boldsymbol{r}, \omega)$ and $\phi^{\mathrm{t}}_{yy}(\boldsymbol{r}, \omega)$. Furthermore, as regards the correlation coefficients, obviously the x and y components are everywhere fully correlated, i.e. $|\mu^{\mathrm{t}}_{xy}| = 1$, whereas the correlations between the z and the x and y components are the same as the s and p correlation of the incident wave, i.e. $|\mu^{\mathrm{t}}_{xz}| = |\mu^{\mathrm{t}}_{yz}| = |\mu^{\mathrm{i}}_{xz}|$. Finally, we emphasize that the (average) phase difference between the incident s and p components is irrelevant as regards the degree of polarization of the transmitted field.

We consider first unpolarized illumination ($|\mu^{\mathrm{i}}_{xz}| = 0$). In figure 2 the 3D degree of polarization $P_3(\boldsymbol{r}, \omega)$ is shown, on a semicircle, at a distance $r = 10\ \mu$m from the output aperture ($d = 50$ nm), for probes with opening angles varying from $\alpha = 20°$ to 45°. We observe that when $\alpha = 20°$, the transmitted field is highly polarized. This is due to the considerably higher transmission of the p-polarized light through the aperture as compared to s-polarized light. When the opening angle is increased, the transmission of the s-polarized light increases only slightly. Instead, the transmission of the p-polarized light first decreases for opening angles ranging from $\alpha = 20°$ to 35°, sharply rises for $\alpha = 40°$ and then again decreases for larger α. This behaviour causes the corresponding decreases and increases in the values of $P_3(\boldsymbol{r}, \omega)$ observed in figure 2. The shape of the $P_3(\boldsymbol{r}, \omega)$ curve is primarily determined by the diffraction pattern of the p-polarized light, which dominates over the s-polarized light.

The behaviour of the 3D degree of polarization $P_3(\boldsymbol{r}, \omega)$ as a function of the radial distance from the aperture is shown in figure 3. As before, the illumination is unpolarized and the diameter of the output aperture is $d = 50$ nm, while the tip opening angle is $\alpha = 20°$ in figure 3(a) and $\alpha = 35°$ in figure 3(b). The values of $P_3(\boldsymbol{r}, \omega)$ are shown along four directions specified by the angle θ with respect to the negative y-axis (see figure 1). In figure 3(a), owing to the significantly higher transmission for the p-polarized light than for the s-polarized light, the field is strongly polarized both in the near zone and in the far zone. Instead, in figure 3(b) the intensities of the s- and p-polarized components are of the same order of magnitude, resulting in substantial angular and radial variations in $P_3(\boldsymbol{r}, \omega)$.

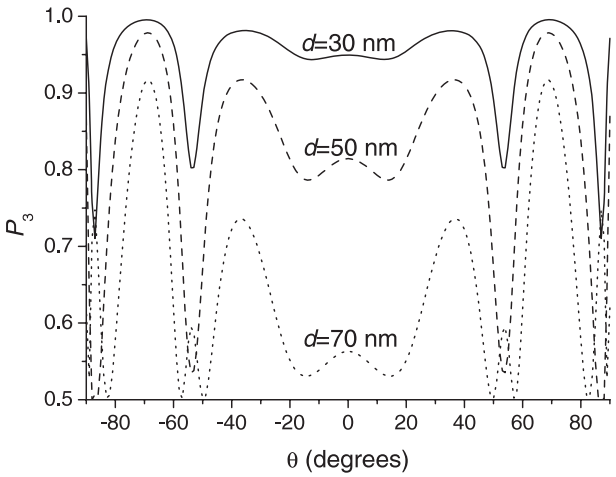

Figure 4. The effect of the aperture width, d, on the 3D degree of polarization, P_3. The incident wave is unpolarized, the tip opening angle is $\alpha = 30°$ and the calculation is carried out for distance $r = 10\ \mu$m.

The effect of the aperture width on the polarization state of the transmitted field is investigated by calculating $P_3(\boldsymbol{r}, \omega)$ (with unpolarized illumination) for three probes with aperture widths $d = 30$, 50, 70 nm (see figure 4). The 3D degree of polarization is observed to be high, when the aperture width is $d = 30$ nm, and to decrease significantly as the aperture width increases. This behaviour is due to the strong dependence of the s-polarized transmission on the aperture width. The intensity of the transmitted s-polarized field becomes comparable to that of the transmitted p-polarized light for $d = 70$ nm. This is seen particularly well in figure 4 for the angles near the forward direction ($\theta \approx 0$), where the y component of the electric field is close to zero and the field behaves as an unpolarized plane wave (in the 2D sense). Thus, the 3D degree of polarization approaches the value $P_3(\boldsymbol{r}, \omega) = 1/2$ when the aperture is increased.

The dependence of the 3D degree of polarization of the transmitted field on the correlation between the orthogonal (s and p) components of the incident wave is depicted in figure 5. The correlation coefficient is, in this case, equal to the 2D degree of polarization $P_2(\boldsymbol{r}, \omega)$, as shown by equation (6). As the value of $|\mu^{\mathrm{i}}_{xz}(\boldsymbol{r}, \omega)|$ of the incident wave increases,

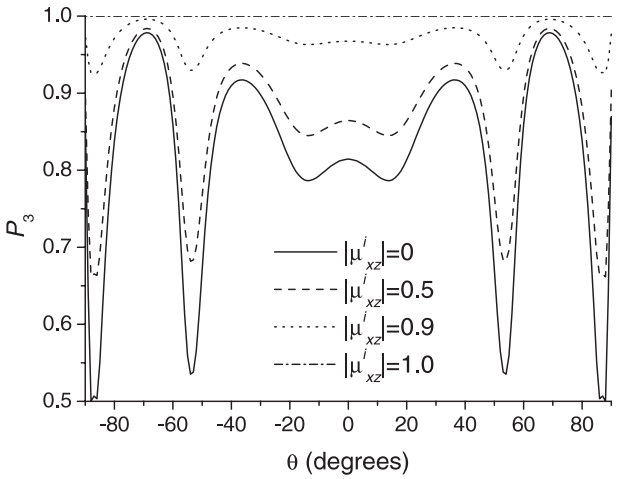

Figure 5. Dependence of the 3D degree of polarization, P_3, on the correlation $|\mu^{\mathrm{i}}_{xy}|$ of the incident field. The opening angle is $\alpha = 30°$ and the calculation is carried out for $r = 10\ \mu$m.

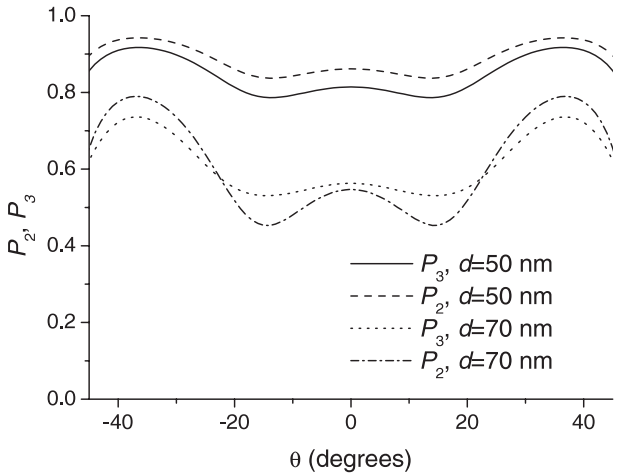

Figure 6. Comparison of the 2D (P_2) and 3D (P_3) degrees of polarization at a distance $r = 10\ \mu$m from the aperture in the far zone. The incident field is unpolarized and the tip opening angle is $\alpha = 30°$.

so does $P_3(\boldsymbol{r}, \omega)$ of the transmitted field. The 3D degree of polarization reaches the maximum value $P_3(\boldsymbol{r}, \omega) = 1$, when the incident field components are fully correlated, i.e. when $|\mu^{\mathrm{i}}_{xz}(\boldsymbol{r}, \omega)| = 1$. This is as expected, since for a fully polarized incident field the transmitted field necessarily is fully polarized as well.

Finally, in figure 6, we compare (with unpolarized illumination) the 2D and 3D degrees of polarization of the transmitted field for two probes having an opening angle $\alpha = 30°$ and aperture widths 50 and 70 nm. In order for $P_2(\boldsymbol{r}, \omega)$ to be a reasonable measure for the degree of polarization, the field must be planar. This requirement is, to a good approximation, satisfied locally at a distance $r = 10\ \mu$m for angles $|\theta| \leqslant 45°$, since the amplitude ratio of the normal and tangential field components on the semicircle centred at the aperture is less than 0.04. Both $P_2(\boldsymbol{r}, \omega)$ and $P_3(\boldsymbol{r}, \omega)$ exhibit similar behaviour showing minima and maxima at the same positions. The difference is their numerical value; a fact that was discussed in section 2.

5. Conclusions

We have analysed the changes in the partial polarization of light transmitted through a near-field probe tip by making use of the concept of the three-dimensional degree of polarization and by applying the boundary-integral method. We examined the dependence of partial polarization on both the opening angle and the aperture size of the tip, and found that the probe can induce significant modifications to the degree of polarization of the illuminating wave. These changes are related to the higher transmission of the p-polarized light as compared with that of s-polarized light through the tip. For instance, a probe with a small opening angle and a small aperture acts like a polarizer blocking the s component and thus resulting in a high degree of polarization for the transmitted field. Furthermore, within the two-dimensional model geometry, we demonstrated that the 2D and 3D formalisms for treating the polarization state of the field provide similar information in the far zone. Comparisons cannot be made in the near zone where the usual 2D description of polarization is not valid. Knowledge of the probe-induced changes in partial polarization of the field is expected to be particularly useful in near-field microscopy and polarization imaging.

Acknowledgments

The authors acknowledge financial support from the Academy of Finland, and ATF also from the Swedish Research Council.

References

[1] Paesler M A and Moyer P J 1996 *Near-Field Optics: Theory, Instrumentation and Applications* (New York: Wiley)
[2] de Fornel F 2001 *Evanescent Waves* (Berlin: Springer)
[3] Martin O J F, Girard C and Dereux A 1995 *Phys. Rev. Lett.* **74** 526
[4] Girard C and Dereux A 1996 *Rep. Prog. Phys.* **59** 657
[5] Tanaka K, Tanaka M and Omoya T 1998 *J. Opt. Soc. Am.* A **15** 1918
[6] Kelso C M, Flammer P D, DeSanto J A and Collins R T 2001 *J. Opt. Soc. Am.* A **18** 1993
[7] Nesci A, Dändliker R, Salt M and Herzig H P 2002 *Opt. Commun.* **205** 229
[8] Grosjean T and Courjon D 2003 *Phys. Rev.* E **67** 046611
[9] Martin O J F, Girard C and Dereux A 1996 *J. Opt. Soc. Am.* A **13** 1801
[10] Greffet J-J and Carminati R 1997 *Prog. Surf. Sci.* **56** 133
[11] Lévêque G, Colas des Francs G, Girard C, Weeber J C, Meier C, Robilliard C, Methevet R and Weiner J 2002 *Phys. Rev.* E **65** 036701
[12] Mandel L and Wolf E 1995 *Optical Coherence and Quantum Optics* (Cambridge: Cambridge University Press)
[13] Born M and Wolf E 1999 *Principles of Optics* 7th edn (Cambridge: Cambridge University Press)
[14] Setälä T, Shevchenko A, Kaivola M and Friberg A T 2002 *Phys. Rev.* E **66** 016615
[15] Wiersig J 2003 *J. Opt. A: Pure Appl. Opt.* **5** 53
[16] Knipp P A and Reinecke T L 1996 *Phys. Rev.* B **54** 1880
[17] Ram-Mohan L and Ramdas L 2002 *Finite Element and Boundary Element Applications in Quantum Mechanics* (Oxford: Oxford University Press)